UPP affects chloroplast development by interfering with chloroplast proteostasis

Vanessa Scherer[1], Leo Bellin[1], Serena Schwenkert[2], Martin Lehmann[2], Jannis Rinne[3], Claus-Peter Witte[3], Kathrin Jahnke[4], Andreas Richter[4], Tobias Pruss[1], Anne Lau[1], Dario Leister[2], Torsten Möhlmann[1]

[1]Plant Physiology, Faculty of Biology, University of Kaiserslautern, Erwin-Schrödinger-Straße, D-67663 Kaiserslautern, Germany

[2]Plant Sciences, Faculty of Biology, Ludwig-Maximilians-University Munich, Großhaderner Straße 2-4, 82152, Planegg-Martinsried, Germany.

[3]Department of Molecular Nutrition and Biochemistry of Plants, Leibniz Universität Hannover, Hannover 30419, Germany

[4]Physiology of Plant Metabolism, Institute for Biosciences, University of Rostock, Albert-Einstein-Strasse 3, 18059, Rostock, Germany

Author for contact:

Dr. Torsten Möhlmann, University of Kaiserslautern, Plant Physiology,

postbox 3049, D-67653 Kaiserslautern, Germany,

Email: t.moehlmann@rptu.de

running head: UPP affects chloroplast proteostasis

Abstract

Arabidopsis uracil phosphoribosyltransferase (UPP) has been identified as an essential protein with a previously unknown moonlighting activity. By analysis of UPP amiRNA mutants, we first confirmed a vital function of UPP in chloroplast development and growth which seems unrelated to nucleotide homeostasis since nucleotide levels were not altered in the mutants. Impaired photosynthesis and reductions in carbohydrate contents in these mutants resulted in an inability to induce flavonoid biosynthesis after high light (HL) treatment. Additionally, levels of raffinose, proline and fumarate, acting as osmoprotectants and carbon-stores were reduced as well. Proteomic analysis suggests a role of UPP in chloroplast proteostasis, particularly under HL, and this was confirmed by immunoblots. PetC, the iron-sulfur protein of the Cytb6f complex, was identified as putative UPP target that is massively reduced in UPP knock-down and knock-out plants, resulting in blocked photosynthetic electron transport, seen by increased unregulated energy dissipation and subsequent damage to the D1 protein of PSII. Proteases, including thylakoid-bound FtsHs, were up-regulated together with components of the chloroplast protein import machinery. We hypothesize that the UPP assists in the targeting of PetC and further interacting proteins to the thylakoid and when this mechanism is impaired in corresponding mutants chloroplast proteases are upregulated as a countermeasure.

Introduction

Nucleotides are organic molecules that are essential compounds of our genetic material and play prominent roles in many cellular processes. Many metabolic enzymes driving nucleotide metabolism are highly conserved among organisms ranging from bacteria to eukaryotes (Peregrin-Alvarez et al., 2009). Thereby, the *de novo* synthesis and catabolism of the two molecule classes, the purines and the pyrimidines, are mostly separated in terms of the enzymes involved (Henderson and Paterson, 1973; (Zrenner et al., 2006; Witte and Herde, 2020). However, to allow for proper nucleic acid synthesis, purines and pyrimidines need to be balanced (Bellin et al., 2023). This is achieved by transcription factors, allosteric regulation and feedback inhibition (Lane and Fan, 2015; Bellin et al., 2021). The salvage pathway recycles nucleosides and nucleobases, helping to balance the nucleotide pool.

There are two pyrimidine salvage pathways in plants. One is active in the cytosol and comprises five uridine-cytidine kinase (UCK) isoforms in Arabidopsis. This pathway mainly contributes to the recycling of pyrimidine nucleosides *in vivo* (Ohler et al., 2019). A second uracil recycling pathway is located in the chloroplast and is initially driven by a single isoform of uracil phosphoribosyl transferase (UPRT or UPP). Arabidopsis recombinant UPP converts uracil along with phosphoribosylpyrophosphate to uridine monophosphate (UMP) whereas *UPP* knockout mutants (*upp*) are devoid of any UPRT activity (Mainguet et al., 2009; Ohler et al., 2019). The functionality of uracil salvage *in vivo* was demonstrated by 5-fluorouracil toxicity and consequential resistance of mutants with reduced UPRT activity (Ohler et al., 2019). Surprisingly, seedling lethal upp-1 can be rescued by complementation with nearly catalytic inactive UPP but not with a highly active homolog from *E. coli*. This, is agrees with other results and suggests that an unknown second function is responsible for the inability of *upp-1* to establish photosynthesis (Mainguet et al., 2009; Arrivault, 2019; Ohler et al., 2019).

Photosynthesis is a dominant process in green plant tissues and chloroplasts have their own machinery for transcription and translation of a number of photosynthesis genes. It is therefore not surprising that nucleotide metabolism mutants that exhibit nucleotide limitation also affect photosynthesis. Examples include knock-down mutants targeting aspartate transcarbamoylase (ATC), which catalyze the first committed step in pyrimidine *de novo* synthesis, CTP-synthase 2 (CTPS2) which catalyzes the final step in the same pathway, as well as thymidine kinase 1b (TK1b) and double knock-

29 out mutants for uridine-cytidine kinase (UCK) 1 and 2 (Clausen et al., 2012; Ohler et al., 2019; Bellin
30 et al., 2021; Bellin et al., 2021). Rescue of ATC and CTPS mutants by nucleotide precursors supports
31 nucleotide limitation as the origin of the observed effects on photosynthesis.

32 However, previous work provided evidence for a moonlighting function of Arabidopsis UPP of
33 so far unknown nature (Ohler et al., 2019). Interestingly, the two downstream enzymes plastid UMP
34 kinase (PUMPKIN) and nucleoside diphosphate kinase 2 (NDPK2) also exhibit moonlighting functions
35 (Dorion and Rivoal, 2015; Arrivault, 2019; Schmid et al., 2019). Since knock-out mutants of both
36 enzymes are not seedling lethal, as it is the case with UPP, these moonlighting functions are most likely
37 distinct from those of UPP.

38 In this work, we generated a series of *UPP-amiRNA* lines with different levels of UPP transcript
39 and protein. Nucleotide quantification revealed wild-type-like levels in one line that otherwise showed
40 a 50% reduction in fresh weight. Using transcriptomics and proteomics, distinct effects on pathways
41 involved in chloroplast protein homeostasis were identified, leading to the hypothesis that the UPP itself
42 is involved in corresponding pathways. PetC was identified as putative target, explaining an observed
43 block in photosynthetic electron transport (PET), PSII damage and increased thylakoid filamentation
44 temperature sensitive (FtsH) metalloprotease levels.

45

46

47 **Results**

48 ***UPP amiRNA* lines show reduced growth although nucleotide levels are wild-type like**

49 *UPP amiRNA* lines were generated exhibiting reduced amounts of UPP transcript. Three lines, *ami-upp-*
50 *1*, *ami-upp-4 and ami-upp-7,* with 54, 34, and 4.6% of wild type (Col-0) transcript levels were used for
51 further analysis. Impaired growth was accompanied by reductions in fresh weight of these mutants after
52 six weeks of growth on soil which correlated well with the lowered *UPP* transcript (Figure 1A, B).
53 Quantification of protein levels with a specific antibody (Ohler et al., 2019) allowed to determine
54 reduced UPP amounts of 97, 7, 13, 11, 2 and 2 % compared to Col-0 for *ami-upp-1*, *-3*, *-4*, *-5*, *-6* and
55 *ami-upp-7*, respectively (Figure 1C). In the following, we will only concentrate on *ami-upp-1*, *ami-upp-*
56 *4*, *ami-upp-7* and a complementation line expressing *UPP* under control of the ubiquitin 10 promoter in
57 *upp-1* (knock-out) background (UBQ10::UPP, Ohler et al., 2019) here denominated as UPP-OX.

58 UPP is an active enzyme in pyrimidine salvage and exhibits a moonlighting function (Ohler et
59 al., 2019). To challenge this finding, (deoxy)-nucleotide, nucleoside and nucleobase levels were
60 quantified in *ami-upp-4* and UPP-OX. Neither of the nucleotides or related molecules showed marked
61 alterations in a comparison between genotypes. (Figure 1D, Supplemental Figure S1, 2). It is therefore
62 highly unlikely that a direct role of UPP in nucleotide metabolism is fundamental for the distinct growth
63 phenotypes of *amiRNA* mutants. Plants of all genotypes grown at 4°C or in HL (high light, 1000 µmol
64 photons s^{-1} m^{-2}) were included in the analysis. When comparing between conditions, some alterations
65 became apparent as increased levels of purine nucleotides ATP, ADP and dADP in cold-treated plants
66 (Supplementary Figure S1). ADP and dADP increased in HL-treated plants as well and increases in UTP
67 were accompanied by reduced amounts of UDP in these plants (Supplemental Figure S1, 2).

68 **Flavonoid biosynthesis is impaired in high light treated *ami-upp-4* line**

69 When testing the performance of *UPP* mutants in different growth regimes, the typical red leaf
70 coloration after several days of high light treatment was missing in *ami-upp-4* and *-7*. Quantification of
71 anthocyanins showed a 14-fold increase in Col-0 after 4d HL and similar in UPP-OX but only a 7-fold
72 increase in *ami-upp-4* (Figure 2A). Quantification of gene expression of early and late flavonoid
73 biosynthetic genes and corresponding transcription factors (TFs)

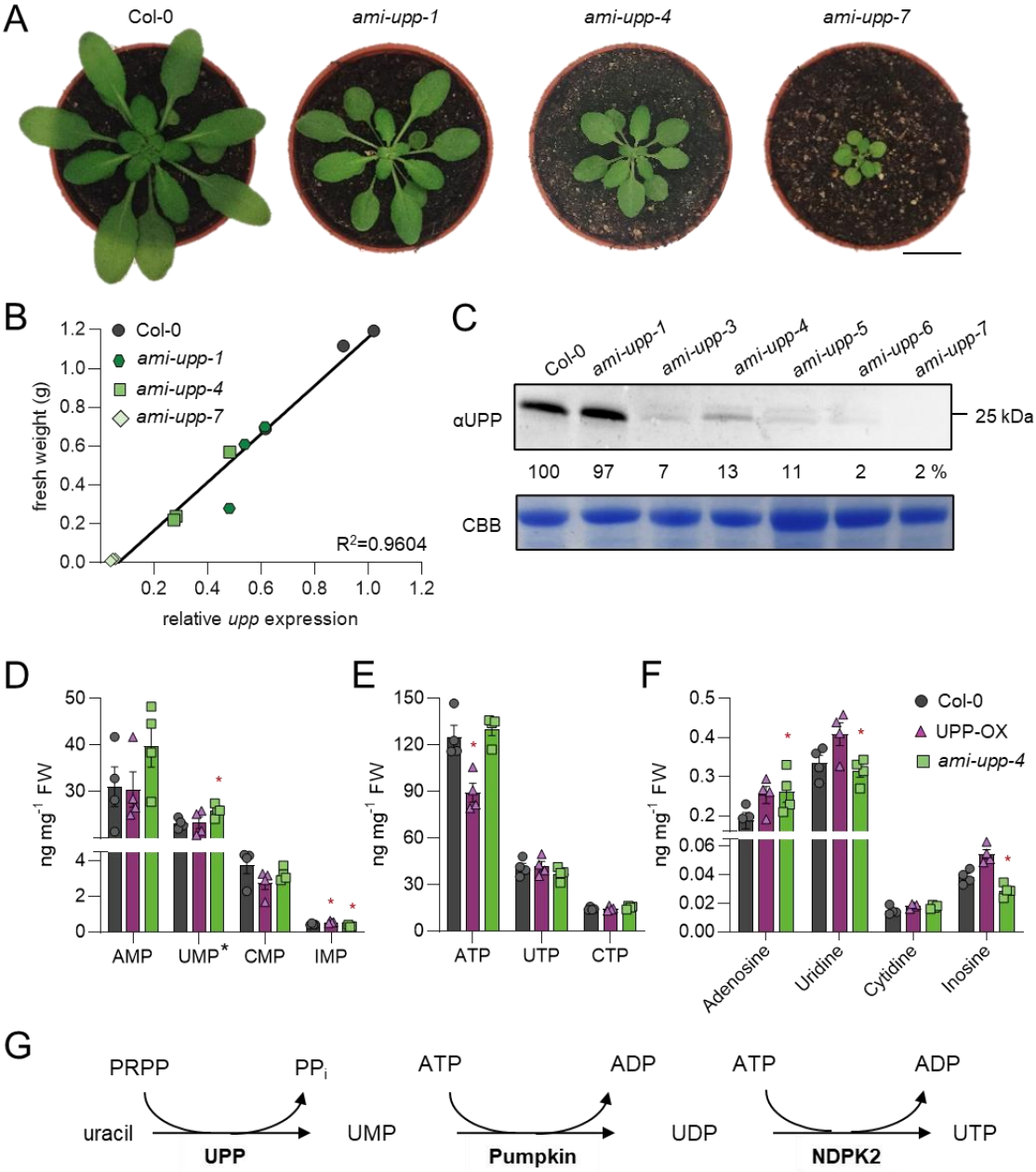

Figure 1. Reduced UPP contents provoke severely impaired plant growth and development. (**A**) Representative five week-old Col-0 and *UPP* knock-down plants (*ami-upp*) grown under a short day regime on soil (10h light/ 14h dark). (**B**) Correlation of relative *upp* expression and fresh weight of five week-old plants (n = 3). (**C**) Western blot detection of UPP amounts with a corresponding quantification in percent to Col-0. Coomassie-brilliant blue (CBB) staining as loading control. (**D**) Nucleotide-monophosphates, UMP*, values for UMP are the sum of free UMP and some UMP released from a low degree of UDP-glucose decay during sample preparation (**E**) nucleotide-triphosphates and (**F**) nucleoside concentrations in five week-old plants. (**G**) Scheme of the uracil salvage pathway in the chloroplast. Plotted are the mean values of biological replicates with the corresponding standard deviation. For statistical analysis one-way ANOVA (**D**, **E**, **F**) was performed followed by Dunnetts's multiple comparison test (* = $p < 0.05$; ** = $p < 0.01$; *** = $p < 0.001$) ($n = 4$). Scale bar in **A** = 2 cm. PUMPKIN, plastidic UMP kinase; NDPK2, nucleoside diphosphate kinase 2 (plastid).

77 (Araguirang and Richter, 2022) revealed significantly reduced induction of transcripts essential for
78 anthocyanin biosynthesis in HL treated *ami-upp-1* and *-4* (Figure 2B). Thereby, the degree of transcript
79 reduction correlated well with reduced UPP expression and growth in corresponding mutants. The
80 reduced expression of PAP1 (Figure 2C), a major TF essential for induction of anthocyanin biosynthetic
81 genes in HL indicated downregulation of sugar related signaling pathways (Zirngibl et al., 2022). When
82 neutral sugars glucose, fructose and sucrose were quantified, significant reductions were observed in
83 HL treated *ami-upp-7*, but not in *upp-ami-4.* (Figure 2C). Both mutants were unable to increase starch
84 levels after HL treatment compared to Col-0 (Figure 2C). Glucose-6-phosphate and fructose-6-
85 phosphate exhibited Col-0 like levels. Phosphoenolpyruvate (PEP), a precursor of the chloroplastic
86 shikimate pathway as well as fumaric acid and raffinose, both relevant for stress responses (Kaplan et
87 al., 2007; Dyson et al., 2016) were reduced in HL treated *ami-upp-4* (Figure 2D).
88

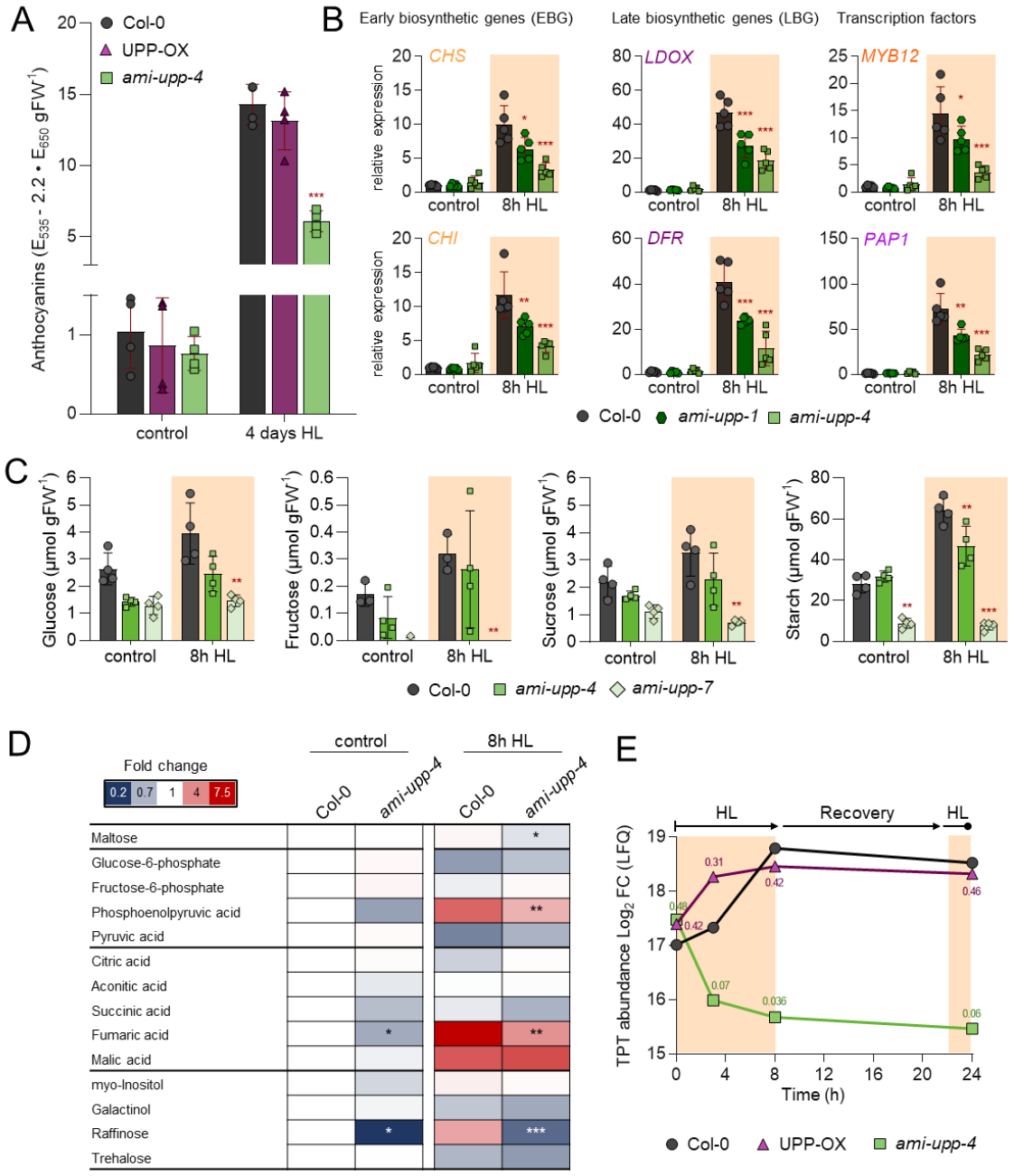

Figure 2. Flavonoid biosynthesis is impaired in *ami-upp* mutants. (**A**) Anthocyanin contents from five-week-old plants after 4 days in high light (HL) compared to control conditions (n = 4). (**B**) Quantification of early (EBGs) and late biosynthetic genes (LBGs) and transcription factors of flavonoid transcript levels in Col-0 and UPP-knockdown Lines (*ami-upp-1* and *ami-upp-4*) after 0h and 8h of HL (1000µmol photons m^{-2} s^{-1}), determined by qRT-PCR (= 5) relative to Col-0 (normalized to actin) (**C**) Glucose, fructose, sucrose and starch contents of Col-0 and UPP-knockdown Lines (*ami-upp-4* and *ami-upp-7*) 0 and 8 hours of HL (n = 4). (**D**) Heat map of the metabolite analysis of Col-0 and *UPP*-knockdown Line (*ami-upp-4*) after 0h and 8h HL, illustrated as fold change of *ami-upp-4* relative to Col-0 under control conditions. Statistical analysis of *ami-upp-4* compared to Col-0 in the same condition. (**E**) Proteome mass spec quantification (Log2 LFQ) of TPT (Triosephosphate phosphate translocator) from a HL time course experiment. P-values of a pairwise comparison to the corresponding Col-0 is shown. Plotted are the mean values of biological replicates with the corresponding standard deviation. For statistical analysis one-way ANOVA (A), two-way ANOVA (**B**, **C**) and students t-test (**D**, **E**) was performed followed by Dunnetts's multiple comparison test (* = p < 0.05; ** = p < 0.01; *** = p < 0.001). -

92 Proteomics analysis, as discussed below in more detail, showed a strong reduction of the triose
93 phosphate-phosphate translocator (TPT) protein levels in *ami-upp-4* after 3h, 8h (more than 8-times
94 less) and 24h of HL exposure (Figure 2E). TPT represents the major export route for photo assimilates
95 and the most prominent membrane protein in the envelope membrane (Flügge, 1999).

96 **Proteomics reveal distinct alterations in proteostasis especially upon HL treatment.**

97 Label free proteomics was chosen as an unbiased method to address UPP's moonlighting function.
98 Whole rosette material of five week-old plants were subjected to HL treatment after 2 hours illumination
99 with ambient light (0h HL). Three hours of HL (3h HL), eight hours HL (8h HL) and subsequent 12
100 hours dark recovery followed by 2h HL (recovery) were tested. The untreated samples showed 104
101 significantly (p-value <0.05, according to pairwise T-test) up and 113 downregulated proteins in *ami-*
102 *upp-4* compared to Col-0 (Figure 3A). This number increased after 3h HL to 151 proteins up and 209
103 proteins down, of which 23% were chloroplast located (Figure 3A, B). The most pronounced increase
104 appeared after 8h HL to 380 up and 303 downregulated proteins of which 27% were chloroplast located
105 (Figure 3A, C). After recovery, still 166 proteins were up and 245 down compared to Col-0 (Figure 3A).
106 A GO-term analysis of the 8h HL proteome performed within the Mapman tool (Thimm et al., 2004),
107 revealed most marked alteration in the categories (Bins) 29 (protein), 20 (stress), 21 (redox) and 16
108 (secondary metabolism) (Figure 3D). Bin 29 (protein) includes 158 proteins with 48 % of differentially
109 expressed proteins (DEPs) in synthesis, followed by degradation (23%), aa activation (10%), targeting
110 (8%), posttranslational modification (4.5%), folding (4.5%) and assembly and cofactor ligation (2%)
111 (Figure 3E).

112 When focusing on individual proteins related to photosynthesis or proteostasis, we found rps12-
113 A (chloroplast ribosomal protein), IPP1 (isopentenyl diphosphate:dimethylallyl diphosphate isomerase),
114 YCF4 (photosystem assembly factor), OEP80 (outer envelope protein 80) upregulated (Figure 2C). In
115 contrast, TPT, UPP, RPP2D (ribosomal protein), GDH2 (mitochondrial glycine cleavage system H-
116 protein), PetC (Rieske FE-S Protein), PsbQ2 (small PSII protein), and FUM2 (cytosolic fumarate
117 hydratase involved in cold and high light acclimation) were down regulated after 8h HL (Figure 3C).

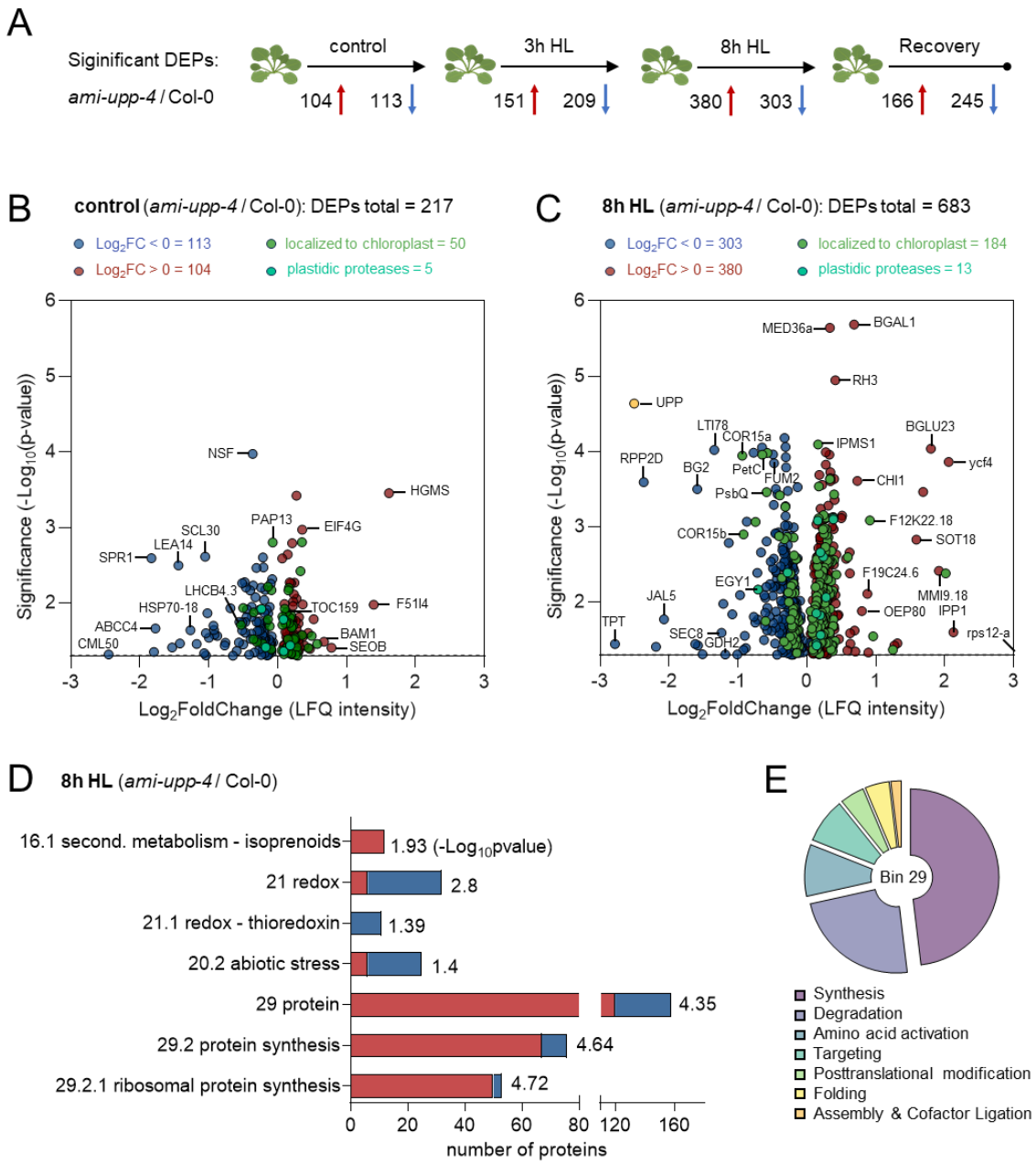

118

119

Figure 3. Proteomics reveal distinct alterations in proteostasis under high light stress. (**A**) Proteome analysis of different expressed proteins (DEPs) in *ami-upp-4* compared to Col-0 under control, three and eight hours of high light (1000µmol photons m^{-2} s^{-1}) and 16h recovery ($p < 0.05$). Plants were grown for five weeks grown under a short-day regime on soil (10h light/ 14h dark). (**B, C**) Volcano plots show DEPs ($p < 0.05$) in *ami-upp-4* compared to Col-0 under control (**B**) and after eight hours high light treatment (**C**). Proteins localized to the chloroplast are highlighted in dark green and plastidic proteases in bright green. (**D**) GO-term analysis of eight hours high light was mapped in Mapman bins ($p < 0.05$) and bin number 29 is further subdivided (**E**). For statistical analysis Students t-test (**A**, **B**, **C**) was performed followed by Dunnetts's multiple comparison test (* = $p < 0.05$; ** = $p < 0.01$; *** = $p < 0.001$).

120

121 Highly abundant protein groups comprise those of electron transport reactions, chloroplast protein
122 import and folding, and proteases (Figure 4). Additional groups comprise ribosomal proteins, redox
123 processes, CBB (Calvin-Benson-Bassham cycle) (Supplemental Figure 3). Among photosynthesis
124 proteins at the thylakoid membrane, those of light harvesting complexes, PSII subunits and $Cytb_6f$
125 subunits were mostly reduced, whereas those of ATP-synthase, NDH (NAD(P)H dehydrogenase
126 subunits involved in cyclic electron flow) and FNR (Ferredoxin $NADP^+$ reductase) were increased
127 (Figure 4A). Several components of chloroplast protein import were altered as well. For example,
128 proteins of the Toc (translocon of outer chloroplast envelope) complex Toc33, Toc159 and Toc75-3 were
129 increased, as well as Tic110 (translocon of inner chloroplast envelope 110) as part of the translocon of
130 the inner chloroplast envelope (Figure 4B). Chaperones of the HSP (heat shock protein) family and
131 CPN60 (chaperonin 60) family were altered after different times in HL. OEP (outer envelope protein)
132 161 and 163 were reduced together with a factor (Akr2) mediating import of outer envelope membrane
133 proteins (Bae et al., 2008).

A **Electron transport reactions**

Fold change: -0.65 -0.4 0 0.15 0.3

		ami-upp-4 / Col-0 0h	3h	8h	Rec.
AT2G34430	Lhcb1.4			*	
AT2G40100	Lhcb4.3	*	*		
AT1G15820	Lhcb6/CP24	*			
AT3G50820	PsbO2		*	*	
AT1G14150	PsbQ			*	
AT4G05180	PsbQ2			***	
AT3G01440	PsbQfamily				**
AT1G06680	PsbP1			**	
AT3G55330	PsbPlike				*
AT5G66570	PsbO1			**	
ATCG00430	PsbG			**	
AT1G34000	Ohp2			*	**
AT3G16140	PsaH	*			
AT1G03130	PsaD2			*	
ATCG00540	PetA		*		
AT4G03280	PetC		**	***	***
AT1G76100	PetE1		*		
AT4G32260	Atp			**	
AT4G04640	AtpC1			**	
AT4G09650	AtpD				**
ATCG00130	AtpF			*	
AT1G20020	FNR2			**	
AT5G66190	FNR1			*	
ATCG01110	NdhH	*		*	
ATCG01090	NdhI			**	
AT1G74880	NdhO				*
AT3G15840	PifI		*		

B **Chloroplast protein import and folding**

Fold change: -0.4 -0.2 0 0.4 0.8

		ami-upp-4 / Col-0 0h	3h	8h	Rec.
AT1G02280	Toc33			**	
AT4G02510	Toc159	*		**	
AT3G46740	Toc75-3			**	
AT5G16620	Tic40			*	
AT1G06950	Tic110			**	
AT2G47840	Tic20-II				*
AT4G35450	Akr2			**	*
AT2G28900	OEP161		*	*	*
AT2G42210	OEP163		*		
AT2G43950	OEP37			*	*
AT3G17970	OEP64			**	
AT5G19620	OEP80			*	
AT4G01800	cpSecA1/ Agy1			**	
AT4G24280	Hsp70-6		**		*
AT5G49910	Hsp70-7		**		
AT5G56030	Hsp90-2			*	
AT2G28000	Cpn60a1				*
AT1G55490	Cpn60b1		*		*
AT3G13470	Cpn60b2	*			

C **Chloroplast proteases**

Fold change: -0.7 -0.35 0 0.2 0.4

		ami-upp-4 / Col-0 0h	3h	8h	Rec.
AT5G42390	SPP			**	
AT3G19170	Prep1			***	**
AT1G73990	SppA			***	*
AT5G35220	Amos1 / Evr3			**	
AT1G50250	FtsH1			**	
AT2G30950	FtsH2 / var2		*		
AT5G42270	FtsH5 / var1			**	
AT1G06430	FtsH8		*		
AT3G27925	DegP1	*		**	
AT2G47940	DegP2			***	
ATCG00670	ClpP1	*		**	
AT1G11750	ClpP6	*		*	
AT1G49970	ClpR1			*	*
AT1G12410	ClpR2				**
AT4G17040	ClpR4			*	
AT5G50920	ClpC1	*	*	*	***
AT3G48870	ClpC2		*		*
AT4G25370	ClpT1				**
AT4G12060	ClpT2				*
AT3G05350	APP2			*	

Figure 4. Proteome mass spec analysis reveals alterations in plastidic proteins in *ami-upp-4* mutants upon high light treatment. (**A**, **B**, **C**) Comparison of protein alterations between Col-0 and *ami-upp-4* associated to electron transport reactions (**A**), chloroplast protein import and folding (**B**) and chloroplast proteases (**C**) ($p < 0.05$). Plants were grown for five weeks grown under a short-day regime on soil (10h light/ 14h dark). For statistical analysis students t-test (**A**, **B**, **C**) was performed followed by Dunnetts's multiple comparison test (* = $p < 0.05$; ** = $p < 0.01$; *** = $p < 0.001$).

137 In contrast, OEP64 and OEP80 (an essential protein paralogue to Toc75, (Hsu et al., 2012)) were
138 increased in amount after 8h HL. From the cpSec1 (chloroplast secretory translocase 1) pathway of ATP
139 driven import of nuclear encoded proteins into thylakoids, the motor protein spSecA1 was upregulated
140 (Figure 4B).

141 Several chloroplast proteases were found altered as well. After 8h HL stromal and thylakoid
142 processing peptidases SPP, SPPA and Prep1 (presequence peptidase 1) were increased similar to
143 thylakoid bound FtsH (filamentation temperature sensitive-H) 1 and 5 (= variegated1, var1) (Figure 4C).
144 DEGP1 (degradation of periplasmic proteins 1) and 2 were reduced whereas members of the Clp
145 (caseinolytic protease) family were mostly increased after 8h HL or recovery. Egy1 metalloprotease is
146 required for grana development and markedly decreased after 8h HL (Figure 4C).

147 **Chloroplast protein synthesis is impaired in *ami-upp* mutants**

148 As numerous changes in the chloroplast proteome were detected, we quantified the steady-state levels
149 of selected photosynthesis-related proteins by immunoblotting. Even under control conditions, several
150 photosynthetic genes such as PsbA (D1), PsbD, PetB, PetC (Rieske), PsaD and LHCBII were
151 downregulated in *ami-upp-4* compared to Col-0 (Figure 5A). Only PC (plastocyanin) and PsaA were
152 detected at higher levels in ami-upp-4. Surprisingly, several proteins were increased in *ami-upp-7*
153 whereas they were down in *ami-upp-4* (PsbA, PetB, PsaD) Maybe, *ami-upp-7* is responding differently
154 to the (very pronounced) reductions of UPP levels which lead to severely reduced growth. The observed
155 accumulation of (non-functional?) photosynthetic proteins may be a result of this. When UPP was
156 overexpressed, higher signals for PsbQ, PC and PsaA and lower signals for PsbD, PetB, PsaD and Tic110
157 were detected (Figure 5A, left). After four hours of high light, all photosynthetic proteins in Col-0
158 decreased or remained unchanged. Notably, most of the detected proteins increased in UPP-OX
159 compared to Col-0 under HL. *Ami-upp-4* and *-7* accumulate higher levels of most photosynthetic
160 proteins and Tic110 compared to Col-0 under high light. Only PsaD and LHCBII are found at lower
161 levels in UPP knockdown plants (Figure 5A, right).

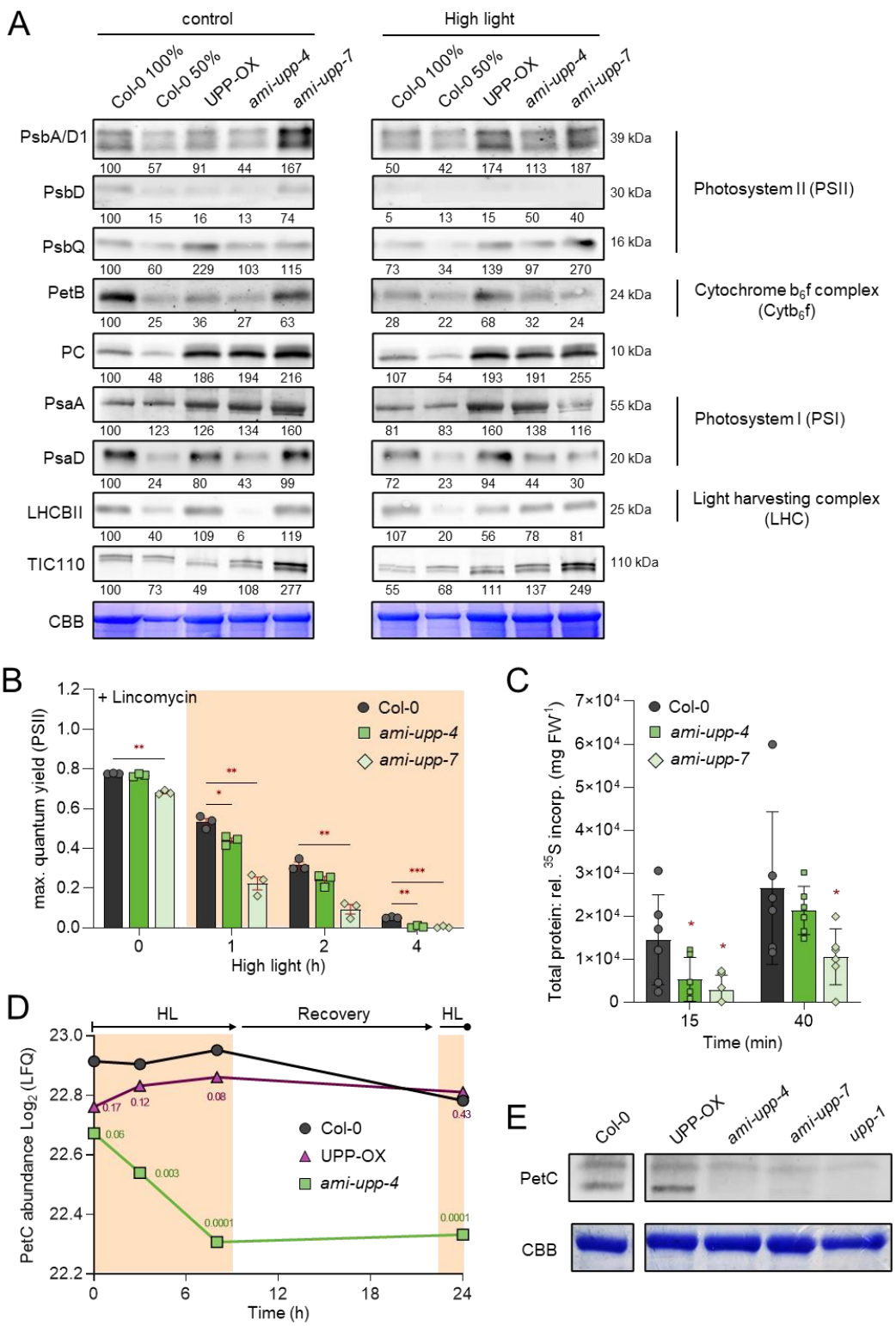

Figure 5. Photosynthetic proteins are reduced and proteostasis is disturbed in *ami-upp* mutants. (**A**) Immunoblot of photosynthesis proteins in leaves of 5-week-old plants after 4 hours of normal light or 4 hours of HL (1000µmol photons m^{-2} s^{-1}). (**B**) Maximum quantum yield of PSII of leaves from Col-0 and UPP-knockdown Lines (*ami-upp-4* and *ami-upp-7*) supplemented with 2.5µM Lincomycin and illuminated with HL. (**C**) *In vivo* radiolabelling of chloroplast proteins in leave discs of Col-0 and UPP-knockdown Lines (*ami-upp-4* and *ami-upp-7*) (n = 6). (**D**) mass spec data as Log2 LFQ of PetC (Rieske iron-sulfur protein) of Col-0, UPP- overexpressing Line UPP-OX and UPP-knockdown Line (*ami-upp-4*). (**E**) Immunoblot of PetC in Col-0, UPP-knockout (*upp-1*) and UPP-knockdown Lines (*ami-upp-4* and *ami-upp-7*) from 7-day-old seedlings. CBB (Coomassie-brilliant blue) staining as loading control. For statistical analysis two-way ANOVA (**B**, **C)** and Students t-test (**D**) was performed followed by Dunnetts's multiple comparison test (* = $p < 0.05$; ** = $p < 0.01$; *** = $p < 0.001$).

163 Since we observed reduced levels of plastid-encoded photosynthetic proteins, the translation efficiency
164 in this organelle was quantified in two independent setups. First, chloroplast translation was blocked by
165 lincomycin and, after overnight incubation in the dark, high light was applied for a further 4h and the
166 photosynthetic efficiency (Fv/Fm) was determined by pulse amplitude modulation (PAM). Fv/Fm was
167 significantly reduced in *ami-upp-7* at all time points and in *ami-upp-4* at 1h and 4h HL (Figure 5B).
168 Second, ^{35}S labelling of newly synthesized proteins in leaf discs of five-week-old plants was followed
169 over 40 min and the activity in total labelled proteins was quantified. Both *ami-upp-4* and *-7* showed
170 significantly lower incorporation after 15 min of labelling and *ami-upp-7* additionally after 40 min
171 (Figure 5B). The results of both experiments indicate that chloroplast translation is reduced when UPP
172 levels are low.

173 **PETC levels are reduced and thylakoid located FtsH proteases are up in *ami-upp* mutants**

174 PetC appeared to be less abundant in the *ami-upp-4* proteome after 3h and 8h HL and after dark recovery
175 compared to Col-0 and UPP-OX (Figure 5D). This aroused our interest because PetC was also identified
176 as a putative UPP interaction partner in the Arabidopsis interactome (Arabidopsis Interactome Mapping,
177 2011). However, chloroplast fractionation, no signal for UPP was detected in the thylakoids by
178 immunoblot, although UPP exhibits a putative twin arginine motif (Supplemental Figure S4). When
179 protein levels were checked by immunoblot, PetC levels were indeed massively reduced in leaf samples
180 from *ami-upp-4* and *-7* as well as in UPP knockout seedlings (Figure 5E). Reduced PetC levels were
181 accompanied by increased levels of the thylakoid-bound FtsH proteases FtsH1, 2, 5, and 8 in
182 immunoblots in control condition as well as after 3h and 8h HL in good agreement with the
183 corresponding proteome analysis. In the latter, UPP-OX showed wild-type-like levels (Figure 6A, B;
184 Supplemental Table S1). FtsH proteases play a crucial role in the D1 repair cycle by removing damaged
185 D1 protein from the PSII core for degradation. After 8h HL, PsbA levels were increased, most strongly
186 in *ami-upp-4*, whereas *ami-upp-7* lacked comparable signals. UPP levels were reduced by HL treatment
187 in all genotypes.

188 These changes in photosynthetic core proteins will ultimately affect photosynthetic
189 performance, as previously described (Mainguet et al., 2009; Ohler et al., 2019). When reinvestigating

photosynthetic parameters in leaves, impaired yield (YII) was observed in *ami-upp-4* and -*7*, compared to Col-0 and UPP-OX (Figure 6 C).

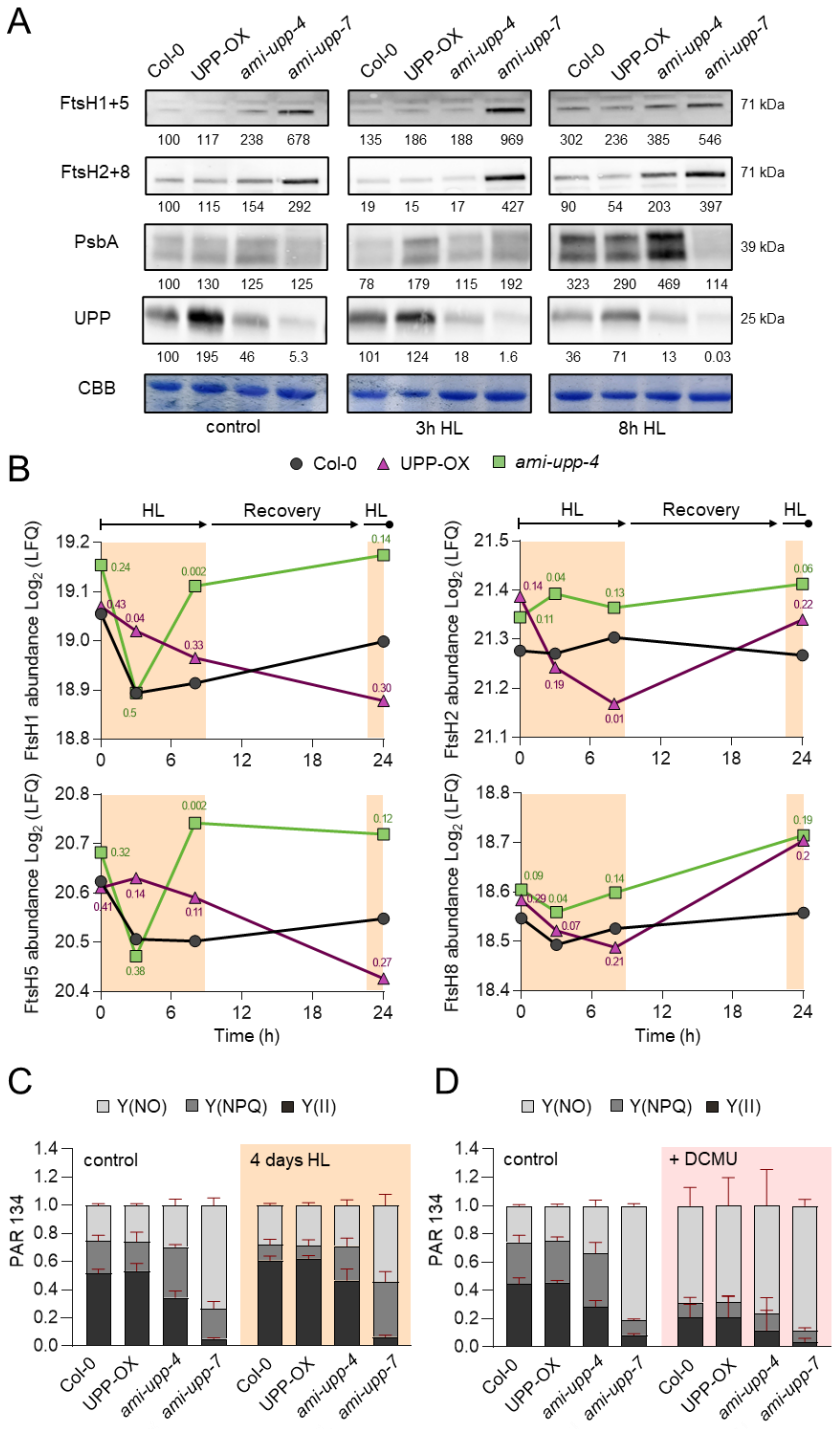

Figure 6. Plastidic proteases are upregulated in *ami-upp* mutants. (**A**) Westernblot detection of proteins involved in proteostasis after normal and high light (1000µmol photons m^{-2} s^{-1}), with a corresponding Coomassie-brilliant blue staining (CBB) as loading control. (**B**) Proteomic data as Log_2 LFQ of FtsH proteases 1, 2, 5, and 8 of Col-0, UPP- overexpressing Line UPP-OX and UPP-knockdown Line (*ami-upp-4*). (**C**, **D**) Yield(II), NPQ and NO of Col-0, UPP- overexpressing Line UPP-OX and UPP-knockdown Lines (*ami-upp-4* and *ami-upp-7*) at PAR 134. Shown are measurements under (**C**) control conditions (*n* = 5) compared to plants after 4 days in HL conditions (*n* = 5) and (**D**) leave discs floated in water compared to 90 min in 5µM DCMU (*n* = 3). Plotted are the mean values of biological replicates +/- standard deviation. For statistical students t-test (**B**) was performed.

While *ami-upp-4* compensated by increased NPQ, *ami-upp-7* was not able to do so, and instead unregulated energy dissipation (NO) massively increased by 290 % (Figure 6C). Such high NO levels are similar to those induced by treatment with 3-(3,4-dichlorophenyl)-1,1-dimethylurea (DCMU), an herbicide that blocks electron transport at the Q_b site of PSII (Russell et al. 1995). When Col-0 leaf discs were treated with DCMU, a similar increase in NO was observed as in untreated *ami-upp-7* plants (Figure 6C, D). A further increase in NO was observed in DCMU-treated *ami-upp-4* and -7. Interestingly, NO accumulation was attenuated in both *ami-upp* mutants grown in HL for 4 days compared to control conditions (Figure 6C).

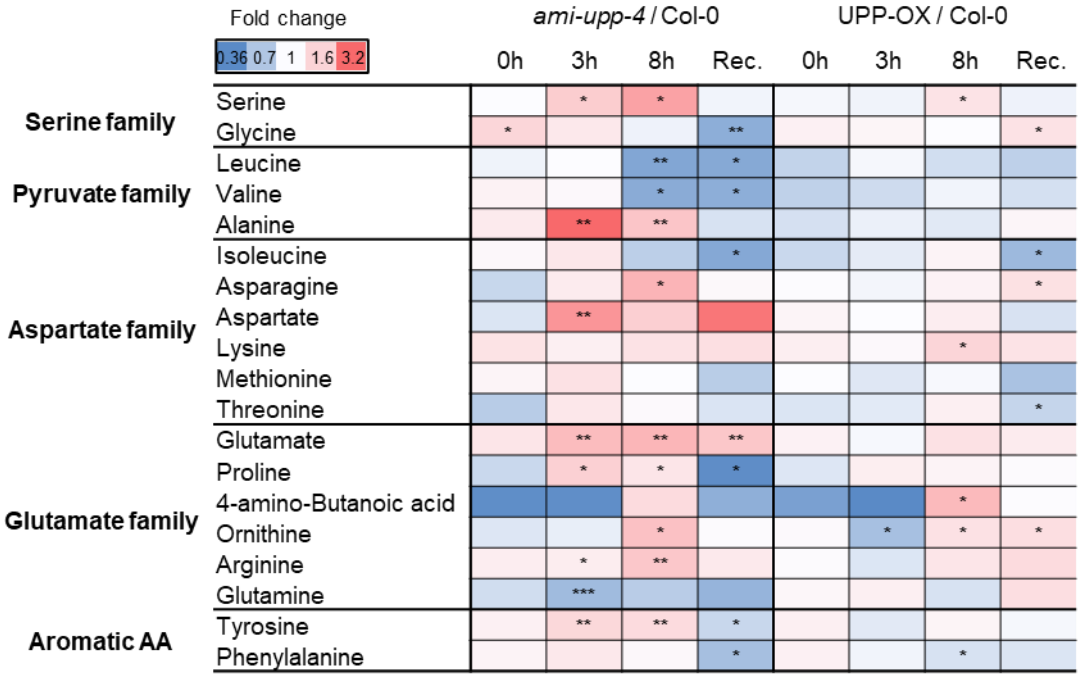

Figure 7. Knock-down of UPP leads to altered levels of free amino acids under HL. (**A**) Heat map of the metabolite analysis of Col-0, UPP-OX and *ami-upp-4* after 0h, 3h and 8h HL and recovery, illustrated as fold change of *ami-upp-4* relative to Col-0 and UPP-OX relative to Col-0 under the same conditions. For statistical analysis and Students t-test was performed followed by Dunnetts's multiple comparison test (* = $p < 0.05$; ** = $p < 0.01$; *** = $p < 0.001$).

Amino acids serve as building blocks for proteins, metabolic precursors, and signaling molecules. Their biosynthesis and degradation vary during plant development and is responsive to stress levels. In general, amino acid levels increase under stress conditions (Häusler et al., 2014; Hildebrandt et al., 2015), and this is also true for the most abundant amino acids, glutamate, glutamine, and aspartate. In our study, amino acids were measured in *ami-upp-4* and UPP-OX mutants under control, 3h and 8h HL

210 and after recovery. The first thing that became apparent was that UPP-OX showed less or no changes in
211 amino acid levels compared to Col-0 (Figure 7). In contrast, *ami-upp-4* showed an increase in seven
212 amino acids after 3 h of high light, which became more pronounced after 8h HL. The highest increases
213 were measured in serine, aspartate, and glutamate. After the night, during the recovery phase, most
214 amino acids decreased again in *ami-upp-4* (Figure 7A, left). The highest increase was observed for
215 alanine after 3h HL (Figure 7).

216

217 Discussion

218 Uracil Phosphoribosyltransferase (UPP) is an essential protein in Arabidopsis as revealed by seedling
219 lethality of knock-out mutants (*upp-1*). Even in the presence of sucrose *upp-1* fails to develop true leaves
220 and cotyledones exhibits smaller chloroplasts and less chlorophyll (Mainguet et al., 2009). *UPP*
221 expression is high in the light and *upp-1* grows like wild type in the dark (Ohler et al., 2019). Altogether
222 it can be stated that UPP is required for the establishment of photosynthesis (Arrivault, 2019; Ohler et
223 al., 2019). Artificial micro-RNA lines generated in the course of this work resemble the *upp-1* phenotype
224 in milder form with respect to photosynthetic efficiency and growth, for example (Figure 1, 6). Thereby,
225 transcript levels, protein amounts and fresh weight correlate well (Figure 1). By complementation
226 analysis with nearly catalytically inactive mutants, a moonlighting function for UPP was established,
227 this means the essential function of UPP is due to a role of the protein independent of its catalytic
228 function (Arrivault, 2019; Ohler et al., 2019). That the main function of UPP is unrelated to pyrimidine
229 metabolism is also indicated by the nearly unaltered levels of pyrimidine nucleotides in the mutant
230 variants compared to the wild type (Figure 1, Supplemental Figure 1, 2). Increased levels of purine
231 nucleotides in cold treated plants of all tested genotypes are in line with previous studies (Savitch et al.,
232 2001; Chen et al., 2023)

233 UPP mutants exhibit obvious alterations in photosynthetic energy dissipation. Whereas *ami-*
234 *upp-4* can compensate reductions in yield (YII) by increased NPQ, the strongest line (*ami-upp-7*) failed
235 to do so and instead increased non-regulated energy dissipation (NO). Surprisingly, high light (HL)
236 treatment led to better yield in *ami-upp-4* and attenuated NO levels in *ami-upp-7* (Figure 6). NO is
237 increased when electron transport is blocked between PSII and the $Cytb_6f$ complex, as it is the case in
238 3-(3',4'-Dichlorophenyl)-1',1'-dimethyl urea (DCMU) treated plants (Russell et al., 1995; Vogel et al.,
239 2012). Thereby, NO levels in *ami-upp-7* grown in control conditions resemble those of DCMU treated
240 Col-0 plants. (Figure 6).

241 A remarkable observation was the inability of *ami-upp-4* and *-7* to accumulate anthocyanins
242 after HL-treatment. When analysing the underlying expression of genes involved in flavonoid
243 biosynthesis, all tested genes were less induced by HL in the mutants compared to Col-0 including
244 corresponding transcription factors Myb12 and Pap1 (Figure 2). This means that flavonoid biosynthesis

245 in our study was not activated by upstream regulatory processes. Such activation by HL occurs by
246 sugars, especially triosephosphates (TP) exported to the cytosol by TPT, as shown recently (Zirngibl et
247 al., 2022). Already after 3h HL and even more pronounced after 8h HL the detectable TPT protein
248 amount in *ami-upp-4* was significantly reduced. It is therefore likely that reduced TP export from the
249 chloroplast and the lack of the inducing sugar-signal is responsible for the reduced anthocyanin
250 biosynthesis in UPP mutants.

251 The reduced photosynthetic efficiency of *ami-upp-4* appears to be largely compensated by
252 reduced growth, as neutral sugars and hexose phosphates were not significantly altered in these plants.
253 However, starch accumulation in HL was significantly reduced (Figure 2). Reduced TPT amounts may
254 function to retract triosephosphates in the chloroplast to prevent depletion of the CBB or to support the
255 oxidative pentose phosphate pathway in the dark. A more than 8-fold reduction of TPT, which is by far
256 the most abundant protein in the chloroplast envelope (Flügge, 1999) can only be achieved by protease
257 activity. To the best of our knowledge this has not been described before. Known envelope proteases are
258 the rhomboid-like proteases RBL10 and RBL11 (Lavell et al., 2019). Whether any of these proteases
259 are involved in the regulation of TPT abundance needs to be addressed in future studies.

260 Besides anthocyanins, raffinose, phoephoenoplpyruvate and fumarate were significantly
261 reduced in *ami-upp-4* under control and HL conditions compared to Col-0 (Figure 2). Increased levels
262 of these metabolites are a typical HL response and this is also reflected in our analysis as well (Garcia-
263 Molina et al., 2020), (Figure 2). Raffinose is an osmoprotectant (Kaplan et al., 2007), and like
264 anthocyanins was increased after HL treatment in Col-0 but not in *ami-upp-4*. It was shown that fumarate
265 and starch can serve as flexible, alternative carbon sinks in Arabidopsis, and that FUM2 is required for
266 fumarate accumulation (Chia et al., 2000; Pracharoenwattana et al., 2010). We observed reduced levels
267 of FUM2 in line with reduced levels of fumarate, possibly to stabilize starch levels in *ami-upp-4*. Proline,
268 like raffinose functions as an osmoprotectant that accumulates during abiotic stress. We observed
269 increased proline levels during acclimation to HL and a normalization during recovery, more
270 pronounced in *ami-upp-4* compared to Col-0 and UPP-OX (Figure 7). Apparently, HL stress is precepted
271 and in case of amino acids increased levels are achieved whereas carbohydrates are limiting, preventing
272 cytosolic accumulation of anthocyanins, raffinose starch and fu marate. It is most likely that the reduced

273 photosynthetic efficiency is responsible for impaired accumulation of these carbon stores. The increase
274 in amino acids during HL may be due to catabolism of damaged proteins, consistent with normalized
275 amino acid levels after recovery accompanied by the synthesis of new proteins.

276 To approach the moonlighting function of UPP, first a GO-term analysis of proteome data was
277 performed with help of the Mapman tool. The 'protein' bin with the sub-categories 'synthesis',
278 'degradation', 'amino acid activation', 'assembly' and 'folding' was the most over-represented functional
279 group (Figure 3). When focusing on chloroplast-located proteins the following ones stood out: RPP2d
280 one of the acidic phosphoproteins of the large SU of the cytosolic 80S ribosome found only in plants
281 (Salih et al., 2020), was most strongly downregulated compared to other proteins. Most other chloroplast
282 or cytosolic ribosomal proteins were upregulated (Figure 3, Supplemental Figure S3) with the highest
283 increase observed for the chloroplast encoded rps12A, which is processed by PPR4 in a higly
284 sophisticated trans-splicing mechanism, which is critical for chloroplast biogenesis and plant
285 development (Lee et al., 2019). Upregulation of other ribosomal proteins was observed upon HL, in
286 contrast to the finding of reduced levels of corresponding transcripts after HL treatment (Garcia-Molina
287 et al., 2020). One could speculate about an attempt to stabilize translation in *ami-upp-4*. However, it
288 appears that chloroplast translation in both, *ami-upp-4* and *-7* was still impaired (Figure 5). Energy
289 limitation due to a block in electron transport could be the cause. Upregulation of chloroplast ATP
290 synthase and components of the cyclic electron transport chain (Figure 4) could be countermeasures
291 taken by the plant.

292 PetC was downregulated in our proteome analysis and in immunoblots in *ami-upp* mutants and
293 *upp-1*. Furthermore, PetC knockout mutants (*petc-2*) show reduced growth, low chlorophyll content, an
294 inability to form NPQ and altered levels of PSII subunits (Maiwald et al., 2003) thus resembling *upp-1*.
295 As PetC has already been identified as an interaction partner of UPP (Arabidopsis Interactome Mapping,
296 2011), we hypothesise that PetC is a target of the UPP function in proteostasis. However, this cannot
297 fully explain the seedling lethal phenotype of *upp-1* because *petc-2* can be propagated on axenic culture
298 in the presence of sucrose, which is not the case for *upp-1* (Maiwald et al., 2003). It is very likely that
299 there are other UPP targets. Nevertheless, the absence of PetC may explain the inability of *ami-upp*
300 mutants to establish NPQ like DCMU treated plants (Figure 4). Such a block in electron transport can

301 cause severe damage to the PSII components, in particular to the D1 protein. In line with this, the
302 observed up-regulation of the thylakoid FtsH proteases Ftsh type A and B in the proteome analysis and
303 immunoblots can be interpreted as an activation of the PSII repair cycle (Kato et al., 2009; Kato et al.,
304 2015). If, as we hypothesize, a block in electron transport is fundamental to D1 damage, then increased
305 repair will not solve the problem and thus activate a continuously increased cycle requiring
306 corresponding FtsH proteases. We observed a high number of altered proteins in redox metabolism,
307 putatively contributing to redox modulation of FtsH activity as observed in Chlamydomonas (Wang et
308 al., 2017). Lumenal Deg-proteases function in the two-step degradation of D1 (Kato et al., 2015) and
309 were down in our HL proteome study, pointing to a direct degradation of D1 by FtsH. The observation
310 of reduced UPP levels in HL exposed plants, even in UPP-OX (Figure 6) might be a consequence of
311 protease mediated degradation and in fact, UPP was identified as a ClpP6 substrate (Sjögren et al., 2006).
312 Components of the chloroplast import machinery like Toc-75, OEP-80- or Tic110, accumulated most
313 likely to increase import of damaged or low abundant proteins like PsbQ, LHCB2, PsaD and PetC. In
314 line with this, late components of protein import apparatus as HSP70, CPN60, and most pronounced
315 processing peptidases SPP, SPPA and Prep1 (Sakamoto et al., 2008) were upregulated.
316 What might be the link between the reduced levels of PetC and the absence of the UPP in our
317 mutants? It is known that PetC is imported into the thylakoids for assembly into the cytochrome b_6f
318 complex via the cpTat or delta pH pathway. However, the import is slow compared to other thylakoid
319 proteins. This is probably due to the need to incorporate the Fe-S cofactor. In addition, PetC is an unusual
320 cpTat substrate as it lacks the typical twin arginine motif (Molik et al., 2001). Before becoming
321 incorporated into the $Cytb_6f$ complex, PetC assembles in complexes together with Cpn60. In our UPP
322 mutants, Cpn60 variants were altered in abundance, and in addition UPP contains an N-terminal twin
323 arginine motif found in most cpTat substrates, but we were unable to identify UPP in isolated thylakoids.
324 We propose that UPP is involved in stabilising PetC while being equipped with Fe-S cluster and/or its
325 subsequent targeting to the thylakoid membrane. Many of the observations discussed above support this
326 view. In this work we could narrow down the role of UPP to chloroplast proteostasis, allowing to design
327 follow-up experiments focusing on the direct molecular and essential function of this enigmatic protein.
328

329 **Materials and Methods**

330 **Plant growth**

331 Plant growth was performed as given in Ohler et al. (2019), with the following additions: normal light
332 120µmol photons m^{-2} s^{-1}, high light 1000µmol photons m^{-2} s^{-1} at 21°C and cold treatment with 4°C.
333 Samples for metabolomics (six independent samples) and proteomics (three independent samples
334 obtained by combining two samples from the metabolomic analysis) were taken form five week-old
335 plants. Total rosette material was harvested and immediately frozen in liquid nitrogen.

336 **Generation of *UPP* knock-down plants**

337 For the generation of UPP (At3g53900) knock-down mutants by gene silencing with artificial
338 microRNA (amiRNA) the protocol of Schwab et al. (2006), was used. Design of amiRNAs targeting
339 UPP was performed using an online tool (www.weigelworld.com). This was used to design different
340 primers with Gateway™-compatible sequences attP1 and attP2 (Supplemental Table S2). Via a BP
341 clonase reaction, all cloned fragments were subcloned into the Gateway™ entry vector pDONR/Zeo
342 and later via an LR clonase reaction into the target vector pK2GW7 downstream of a 35S-CaMV
343 promoter.

344 Transformation of *Arabidopsis thaliana* Wildtype (Col-0) plants was done by floral dip
345 (Narusaka et al., 2010) of previously transformed *Agrobacterium tumefaciens* GV3101 (Furini et al.,
346 1994). Positive transformed plants were first selected on ½ MS agar plates supplemented with
347 Kanamycin and later transferred on soil. By quantification of *upp* transcript levels, different
348 independent lines with 54-4.6% UPP transcript left.

349 **Transcript quantification with qRT PCR**

350 RNA isolation, cDNA preparation and PCR were performed as given in (Ohler et al., 2019) In brief.
351 RNA was isolated from whole plant tissue grinded in liquid nitrogen with the Nucleospin RNA Plant
352 Kit (Macherey-Nagel, Düren, Germany) according to the manufacturer's advice. For transcription of
353 RNA into cDNA the qScript cDNA Synthesis Kit (Quantabio, United States) was used. Transcripts in
354 flavonoid biosynthesis and corresponding primers for qRT-PCR are described in (Zirngibl et al., 2022)
355 and additional primers for UPP are listed in Supplemental Table S2.

356

357 **Quantification of, anthocyanins and metabolites**

358 Plant material of five-week old soil grown plants were used throughout. Anthocyanins were extracted
359 from leaf tissue grinded in liquid nitrogen. 50 mg grinded material was extracted in 1 ml extraction
360 buffer (H2O: 1-propanol: HCL (81:18:1). Samples were boiled at 95 °C for 3 min, incubated in the dark
361 over night at RT and the supernatant was measured photometrically at 535 nm and 650 nm. The
362 extinction was corrected by Rayleigh's formula (E_{535}-2.2E_{650}).

363 For the extraction of sugars and starch 50 mg of leaf tissue grinded in liquid nitrogen. The
364 material was boiled in 500 µL deionized water for 15 min at 95 °C, the supernatant was used for sugar
365 and the pellet was used for starch measurements. Quantification was done photometrically with a NAD^+-
366 coupled enzymatic assay (Stitt et al., 1989).

367 Nucleotide quantification was performed as given in (Straube *et al.*, 2021).

368 Primary metabolite analysis was performed via GC–TOF–MS as described previously in Garcia-Molina
369 et al. (2020). Therefore, 100 mg of fresh plant material was ground and mixed with 180 µl of -20°C cold
370 methanol. Internal standards, namely ribitol (10 µl at 0.2 mg ml^{-1} in water) and 13C-sorbitol (10 µl at
371 0.2 mg ml^{-1} in water), were added to facilitate relative quantification of metabolites. After incubating
372 the mixture at 70°C for 15 minutes, it was combined with 100 µl of chloroform and 200 µl of water. To
373 partition polar and non-polar compounds, the solution underwent a 15-minute centrifugation at 25000 g
374 for phase separation. Fifty µl of the upper (polar) phase was vacuum-dried, resulting in a pellet that was
375 resuspended in 10 µl of methoxyaminhydrochloride (20 mg ml^{-1} in pyridine). This mixture was shaken
376 at 40°C for 90 minutes followed by addition of 20 µl of BSTFA (N,O-
377 Bis[trimethylsilyl]trifluoroacetamide) containing 2.5 µl of a retention time standard mixture of linear
378 alkanes for retention time alignment. The mixture was further incubated at 40°C for another 45 minutes.
379 For GC–TOF–MS analysis, 1 µl of each derivatized sample was injected into a Pegasus HT system
380 (Leco, St Joseph, USA) utilizing an autosampler system (Combi PAL, CTC Analytics AG, Zwingen,
381 Switzerland). Helium gas acted as the carrier, maintained at a constant flow rate of 1 ml min^{-1}. The
382 system utilized an Agilent 7890A oven (Agilent, Santa Clara, USA) with a VF-5ms column (30 m) plus
383 an EZ-Guard column (10 m). The temperature of the split/splitless injector, as well as that of the transfer
384 line and ion source, were set to 250°C. Starting at an initial temperature of 70°C, the oven temperature

385 increased gradually at a rate of 9 °C min^{-1} until it reached the final temperature of 350°C. To prevent
386 solvent contamination, a solvent delay of 340 seconds was implemented. The metabolites were ionized
387 and fractionated using a 70 eV ion pulse. Mass spectra, spanning an m/z range of 35–800, were captured
388 at a frequency of 20 scans per second. Evaluation and interpretation of the collected data, including
389 chromatograms and mass spectra, were conducted using ChromaTOF 4.7 and TagFinder 4.1 software
390 (Luedemann et al., 2008), and the Golm Metabolome Database (Kopka et al., 2005). For details see
391 Supplemental Data S1

392 **Protein extraction**

393 Proteins were extracted on ice from 50 mg samples of whole rosettes frozen and grinded in liquid
394 nitrogen with protein extraction buffer (50 mM HEPES-KOH, pH 7.2, 5 mM $MgCl_2$, 2 mM DTT,
395 0.01% DDM, 1 mM EDTA, and 2 mM phenylmethylsulfonyl fluoride (PMSF)). After sonification, the
396 protein amount of the supernatant was measured with a Bradford Assay and the samples were stored at
397 -80°C until use.

398 **Immunoblotting and western blot detection**

399 Immunoblots were essentially performed as given in (Ohler et al., 2019), here the proteins were
400 separated on SDS-gels and transferred onto a nitrocellulose membrane by the semi-dry Transblot
401 Turbo Transfer System (Bio-Rad, Hercules, CA, USA). Primary antibodies were obtained from
402 Agrisera (Vännäs, Sweden) except for anti-UPP (Ohler et al., 2019).

403 **Pulse-amplitude-modulation (PAM) fluorometry measurements**

404 Photosynthetic activity was measured as described previously (Bellin et al., 2023). Five-week-old
405 plants grown under standard conditions were transferred to high light. DCMU (5µM) treatment was
406 done with leaf discs of respective plants. Five leaf discs were incubated for 90 min in 5ml Buffer with
407 $CaCl_2$ (Russell et al., 1995).

408 **Proteome analysis by mass spectrometry**

409 Total leaf material of five-week-old plants was analyzed in three independent biological replicates.
410 Protein extraction and trypsin digestion were performed as described in (Marino et al., 2019). Liquid
411 chromatography-tandem mass spectrometry (LC-MS/MS) was performed as described previously, but
412 peptides were separated over a 90 min linear gradient of 5–80% (v/v) ACN (Espinoza-Corral et al.,

413 2023). Raw files were processed using the MaxQuant software version 2.1.0.0 (Cox and Mann, 2008).
414 Peak lists were searched against the Arabidopsis reference proteome (Uniprot, www.uniprot.org) using
415 default settings with 'mach-between-runs' enabled. Proteins were quantified using the label-free
416 quantification algorithm (LFQ) (Cox et al., 2014). Downstream analysis was performed using Perseus
417 version 2.0.6.0 (Tyanova et al., 2016). Potential contaminants, proteins identified only by site
418 modification, and reverse hits were excluded for further analysis. Only protein groups that could be
419 quantified by the LFQ algorithm in at least two of the three replicates in at least one condition. LFQ
420 intensities were $\log_2$-transformed and missing values were imputed from a normal distribution with
421 Perseus using standard settings. For details see Supplemental Data S2.

422 **Statistical analyses**

423 Statistical analysis of qRT-PCR, proteomic and metabolomic analysis data was performed using the
424 Student's t-test (see also legend for details). Asterisks indicate statistically significant differences
425 determined using Student's t-test (*$p < 0.05$; **$p < 0.01$, ***$p < 0.001$). The significance criteria for
426 comparisons within the proteomic dataset were based on adjusted $p < 0.05$. Changes in protein levels
427 within a given pairwise comparison were expressed as log2 fold change (log 2 FC), or as fold change
428 (FC) where FC equals the second condition divided by the first condition (Pagano et al., 2023).

429 **^{35}S pulse labelling of proteins in leaves**

430 Labelling of proteins in leaf discs by ^{35}S Methionin/Cystein was performed as given in (DeTar et al.,
431 2021).

432

433 **Supplemental data**

434 Supplemetal Table S1: Primers used in this study

435 Supplemetal Figure S1: (deoxy) nucleotide levels in cold and HL

436 Supplemetal Figure S2: (deoxy) nucleosides and nucleobases in cold and HL

437 Supplemetal Figure S3: proteomics results of functional groups "CBB", "plastidic ribosomes" and
438 "redox"

439 Supplemetal Figure S4: stromal localization of UPP

440 Supplemental Data S1: Complete list of identified metabolites

441 Supplemental Data S2: Complete list of identified proteins

442

443 **Acknowledgement and funding**

444 This work was funded by DFG grants (CRC Transregio TRR175, B06 to S.S. B08 to T.M, C05 to A.R.
445 and C06 to D.L.).

446

447 **Author contributions**

448 T.M. conceived and supervised the study, obtained funding, and provided resources. V.S. generated all
449 mutants and performed characterization, and phenotyping. V.S., L.B. performed analysis and
450 interpretation of proteomic and metabolomic data. S.S. performed and quantified proteomic analysis.
451 M.L. performed and quantified metabolomic data analysis. D.L. supervised proteomics and
452 metabolomics J.R. performed and C.P.W. advised and interpreted nucleotide quantification. K.J.
453 performed and A.R. advised and interpreted expression of flavonoid biosynthesis genes. T.P. supported
454 immunoblotting and quantification A.L. supported results interpretation related to proteostasis. T.M.,
455 V.S. and L.B. wrote the original draft. All authors reviewed and agreed to the final manuscript.

456 **Data Availability statement**

457 The data underlying this article (proteomics) will be made available within the proteomics identification
458 database (PRIDE) upon publication.

459 **Conflicts of interests**

460 No conflicts of interest declared

461

References

Arabidopsis Interactome Mapping Consortium (2011) Evidence for network evolution in an Arabidopsis interactome map. Science **333:** 601-607

Araguirang GE, Richter AS (2022) Activation of anthocyanin biosynthesis in high light - what is the initial signal? New Phytol **236:** 2037-2043

Arrivault S (2019) UMP Pyrophosphorylase: A moonlighting protein with essential functions in chloroplast development and photosynthesis establishment. Plant Physiol **180:** 1779-1780

Bae W, Lee YJ, Kim DH, Lee J, Kim S, Sohn EJ, Hwang I (2008) AKR2A-mediated import of chloroplast outer membrane proteins is essential for chloroplast biogenesis. Nat Cell Biol **10:** 220-227

Bellin L, Del Cano-Ochoa F, Velazquez-Campoy A, Möhlmann T, Ramon-Maiques S (2021) Mechanisms of feedback inhibition and sequential firing of active sites in plant aspartate transcarbamoylase. Nat Commun **12:** 947

Bellin L, Garza Amaya DL, Scherer V, Pruss T, John A, Richter A, Möhlmann T (2023) Nucleotide imbalance, provoked by downregulation of Aspartate Transcarbamoylase impairs cold acclimation in Arabidopsis. Molecules **28**

Bellin L, Scherer V, Dörfer E, Lau A, Vicente AM, Meurer J, Hickl D, Möhlmann T (2021) Cytosolic CTP production limits the establishment of photosynthesis in Arabidopsis. Front Plant Sci **12:** 789189

Chen X, Kim SH, Rhee S, Witte CP (2023) A plastid nucleoside kinase is involved in inosine salvage and control of purine nucleotide biosynthesis. Plant Cell **35:** 510-528

Chia DW, Yoder TJ, Reiter WD, Gibson SI (2000) Fumaric acid: an overlooked form of fixed carbon in Arabidopsis and other plant species. Planta **211:** 743-751

Clausen AR, Girandon L, Ali A, Knecht W, Rozpedowska E, Sandrini MP, Andreasson E, Munch-Petersen B, Piskur J (2012) Two thymidine kinases and one multisubstrate deoxyribonucleoside kinase salvage DNA precursors in Arabidopsis thaliana. FEBS J **279:** 3889-3897

Cox J, Hein MY, Luber CA, Paron I, Nagaraj N, Mann M (2014) Accurate proteome-wide label-free quantification by delayed normalization and maximal peptide ratio extraction, termed MaxLFQ. Mol Cell Proteomics **13:** 2513-2526

Cox J, Mann M (2008) MaxQuant enables high peptide identification rates, individualized p.p.b.-range mass accuracies and proteome-wide protein quantification. Nat Biotechnol **26:** 1367-1372

DeTar RA, Barahimipour R, Manavski N, Schwenkert S, Hohner R, Bolter B, Inaba T, Meurer J, Zoschke R, Kunz HH (2021) Loss of inner-envelope K^+/H^+ exchangers impairs plastid rRNA maturation and gene expression. Plant Cell **33:** 2479-2505

Dorion S, Rivoal J (2015) Clues to the functions of plant NDPK isoforms. Naunyn-Schmiedeberg's archives of pharmacology **388:** 119-132

Dyson BC, Miller MA, Feil R, Rattray N, Bowsher CG, Goodacre R, Lunn JE, Johnson GN (2016) FUM2, a cytosolic fumarase, is essential for acclimation to low temperature in Arabidopsis thaliana. Plant Physiol **172:** 118-127

Espinoza-Corral R, Schwenkert S, Schneider A (2023) Characterization of the preferred cation cofactors of chloroplast protein kinases in Arabidopsis thaliana. FEBS Open Bio **13:** 511-518

Flügge UI (1999) Phosphate translocators in plastids. Annu Rev Plant Physiol Plant Mol Biol **50:** 27-45

Furini A, Koncz C, Salamini F, Bartels D (1994) Agrobacterium-mediated transformation of the desiccation-tolerant plant *Craterostigma-Plantagineum*. Plant Cell Reports **14:** 102-106

Garcia-Molina A, Kleine T, Schneider K, Mühlhaus T, Lehmann M, Leister D (2020) Translational components contribute to acclimation responses to high light, heat, and cold in Arabidopsis. iScience **23:** 101331

512 **Henderson JF, and Paterson ARP** (1973). Nucleotide metabolism: an introduction. Academic Press,
513 New York and London.

514 **Hsu SC, Nafati M, Inoue K** (2012) OEP80, an essential protein paralogous to the chloroplast protein
515 translocation channel Toc75, exists as a 70-kD protein in the *Arabidopsis thaliana* chloroplast
516 outer envelope. Plant Mol Biol **78:** 147-158

517 **Kaplan F, Kopka J, Sung DY, Zhao W, Popp M, Porat R, Guy CL** (2007) Transcript and
518 metabolite profiling during cold acclimation of Arabidopsis reveals an intricate relationship of
519 cold-regulated gene expression with modifications in metabolite content. Plant J **50:** 967-981

520 **Kato Y, Miura E, Ido K, Ifuku K, Sakamoto W** (2009) The variegated mutants lacking chloroplastic
521 FtsHs are defective in D1 degradation and accumulate reactive oxygen species. Plant Physiol
522 **151:** 1790-1801

523 **Kato Y, Ozawa S, Takahashi Y, Sakamoto W** (2015) D1 fragmentation in photosystem II repair
524 caused by photo-damage of a two-step model. Photosynth Res **126:** 409-416

525 **Kopka J, Schauer N, Krueger S, Birkemeyer C, Usadel B, Bergmüller E, Dormann P,**
526 **Weckwerth W, Gibon Y, Stitt M, Willmitzer L, Fernie AR, Steinhauser D** (2005)
527 GMD@CSB.DB: the Golm Metabolome Database. Bioinformatics **21:** 1635-1638

528 **Lane AN, Fan TW** (2015) Regulation of mammalian nucleotide metabolism and biosynthesis.
529 Nucleic Acids Res **43:** 2466-2485

530 **Lavell A, Froehlich JE, Baylis O, Rotondo AD, Benning C** (2019) A predicted plastid rhomboid
531 protease affects phosphatidic acid metabolism in *Arabidopsis thaliana*. Plant J **99:** 978-987

532 **Lee K, Park SJ, Colas des Francs-Small C, Whitby M, Small I, Kang H** (2019) The coordinated
533 action of PPR4 and EMB2654 on each intron half mediates trans-splicing of rps12 transcripts
534 in plant chloroplasts. Plant J **100:** 1193-1207

535 **Luedemann A, Strassburg K, Erban A, Kopka J** (2008) TagFinder for the quantitative analysis of
536 gas chromatography--mass spectrometry (GC-MS)-based metabolite profiling experiments.
537 Bioinformatics **24:** 732-737

538 **Mainguet SE, Gakiere B, Majira A, Pelletier S, Bringel F, Guerard F, Caboche M, Berthome R,**
539 **Renou JP** (2009) Uracil salvage is necessary for early Arabidopsis development. Plant J **60:**
540 280-291

541 **Maiwald D, Dietzmann A, Jahns P, Pesaresi P, Joliot P, Joliot A, Levin JZ, Salamini F, Leister D**
542 (2003) Knock-out of the genes coding for the Rieske protein and the ATP-synthase delta-
543 subunit of Arabidopsis. Effects on photosynthesis, thylakoid protein composition, and nuclear
544 chloroplast gene expression. Plant Physiol **133:** 191-202

545 **Marino G, Naranjo B, Wang J, Penzler JF, Kleine T, Leister D** (2019) Relationship of GUN1 to
546 FUG1 in chloroplast protein homeostasis. Plant J **99:** 521-535

547 **Molik S, Karnauchov I, Weidlich C, Herrmann RG, Klösgen RB** (2001) The Rieske Fe/S protein
548 of the cytochrome b6/f complex in chloroplasts: missing link in the evolution of protein
549 transport pathways in chloroplasts? J Biol Chem **276:** 42761-42766

550 **Narusaka M, Shiraishi T, Iwabuchi M, Narusaka Y** (2010) The floral inoculating protocol: a
551 simplified *Arabidopsis thaliana* transformation method modified from floral dipping. Plant
552 Biotechnology **27:** 349-351

553 **Ohler L, Niopek-Witz S, Mainguet SE, Möhlmann T** (2019) Pyrimidine salvage: physiological
554 functions and interaction with chloroplast biogenesis. Plant Physiol **180:** 1816-1828

555 **Pagano A, Kunz L, Dittmann A, Araujo SS, Macovei A, Shridhar Gaonkar S, Sincinelli F,**
556 **Wazeer H, Balestrazzi A** (2023) Changes in *Medicago truncatula* seed proteome along the
557 rehydration-dehydration cycle highlight new players in the genotoxic stress response. Front
558 Plant Sci **14:** 1188546

559 **Peregrin-Alvarez JM, Sanford C, Parkinson J** (2009) The conservation and evolutionary
560 modularity of metabolism. Genome Biol **10:** R63

561 **Pracharoenwattana I, Zhou W, Keech O, Francisco PB, Udomchalothorn T, Tschoep H, Stitt M,**
562 **Gibon Y, Smith SM** (2010) Arabidopsis has a cytosolic fumarase required for the massive

allocation of photosynthate into fumaric acid and for rapid plant growth on high nitrogen. Plant J **62:** 785-795

Russell AW, Critchley C, Robinson SA, Franklin LA, Seaton G, Chow WS, Anderson JM, Osmond CB (1995) Photosystem II regulation and dynamics of the chloroplast D1 protein in Arabidopsis leaves during photosynthesis and photoinhibition. Plant Physiol **107:** 943-952

Sakamoto W, Miyagishima SY, Jarvis P (2008) Chloroplast biogenesis: control of plastid development, protein import, division and inheritance. Arabidopsis Book **6:** e0110

Salih KJ, Duncan O, Li L, Trosch J, Millar AH (2020) The composition and turnover of the *Arabidopsis thaliana* 80S cytosolic ribosome. Biochem J **477:** 3019-3032

Savitch LV, Barker-Åstrom J, Ivanov AG, Hurry V, Öquist G, Huner NP, Gardeström P (2001) Cold acclimation of *Arabidopsis thaliana* results in incomplete recovery of photosynthetic capacity, associated with an increased reduction of the chloroplast stroma. Planta **214:** 295-303

Sjögren LL, Stanne TM, Zheng B, Sutinen S, Clarke AK (2006) Structural and functional insights into the chloroplast ATP-dependent Clp protease in Arabidopsis. Plant Cell **18:** 2635-2649

Schmid LM, Ohler L, Möhlmann T, Brachmann A, Muino JM, Leister D, Meurer J, Manavski N (2019) PUMPKIN, the sole plastid UMP kinase, associates with group II introns and alters their metabolism. Plant Physiol **179:** 248-264

Schwab R, Ossowski S, Riester M, Warthmann N, Weigel D (2006) Highly specific gene silencing by artificial microRNAs in Arabidopsis. Plant Cell **18:** 1121-1133

Stitt M, Lilley R, Gerhardt R, Heldt HW (1989) Metabolite levels in specific cells and subcellular compartments of plant leaves. Meth. Enzymol **174:** 518-552

Straube H, Niehaus M, Zwittian S, Witte CP, Herde M (2021) Enhanced nucleotide analysis enables the quantification of deoxynucleotides in plants and algae revealing connections between nucleoside and deoxynucleoside metabolism. Plant Cell **33**: 270-289

Thimm O, Blasing O, Gibon Y, Nagel A, Meyer S, Kruger P, Selbig J, Muller LA, Rhee SY, Stitt M (2004) MAPMAN: a user-driven tool to display genomics data sets onto diagrams of metabolic pathways and other biological processes. Plant J **37:** 914-939

Tyanova S, Temu T, Sinitcyn P, Carlson A, Hein MY, Geiger T, Mann M, Cox J (2016) The Perseus computational platform for comprehensive analysis of (prote)omics data. Nat Methods **13:** 731-740

Vogel MO, Gomez-Perez D, Probst N, Dietz KJ (2012) Combinatorial signal integration by APETALA2/Ethylene Response Factor (ERF)-transcription factors and the involvement of AP2-2 in starvation response. Int J Mol Sci **13:** 5933-5951

Wang F, Qi Y, Malnoe A, Choquet Y, Wollman FA, de Vitry C (2017) The High Light Response and Redox Control of Thylakoid FtsH Protease in *Chlamydomonas reinhardtii*. Mol Plant **10:** 99-114

Witte CP, Herde M (2020) Nucleotide Metabolism in Plants. Plant Physiol **182:** 63-78

Zirngibl ME, Araguirang GE, Kitashova A, Jahnke K, Rolka T, Kuhn C, Nagele T, Richter AS (2022) Triose phosphate export from chloroplasts and cellular sugar content regulate anthocyanin biosynthesis during high light acclimation. Plant Commun**:** 100423

Zrenner R, Stitt M, Sonnewald U, Boldt R (2006) Pyrimidine and purine biosynthesis and degradation in plants. Annu. Rev. Plant Biol **57:** 805-836